

Separation and Characterization of Dust and Ground Water Particulates Using Gravitational SPLITT Fractionation

Seungho Lee,* Hee-Young Park, Sang-Keun Lee, Sung-Gwon Yang, and Chul Hun Eum†

Department of Chemistry, Hannam University, Taejon 306-791, Korea

†Korea Institute of Geoscience and Mineral Resources, Taejon 305-350, Korea

Received February 8, 2001

Split-flow thin (SPLITT) cell Fractionation (SF) is a technique that allows separation of particulates and macromolecules into two fractions. A gravitational SF (GSF) system is constructed and tested for its applicability for separation of dust and ground water particulates. When tested with polystyrene latex particles, experimental data were in good agreements with theory. The 9.8 and 21.4 μm polystyrene particles were successfully separated in a continuous mode, where the mixture is continuously fed into the GSF channel allowing separation in a large scale. The GSF system is successfully applied to continuous separation of dust and ground water particles based on the sedimentation coefficient, which is closely related to the particle size. The separations were confirmed by microscopy and energy-dispersive X-ray (EDX) analysis.

Keywords : Gravitation SPLITT Fractionation (GSF), Preparative separation, Sedimentation coefficient, Dust, Ground water particles.

Introduction

Analysis of environmental particulates in air, underground water, or river is important for understanding of the roles played by those particles in environment.^{1,2} It is known that environmental particles, even in very low concentrations (1-100 mg/L), strongly influence the transport and the fate of pollutants of various origin due to their high surface to mass ratio. Analysis of environmental particulates usually requires separation into two or more subpopulations as they are highly polydisperse in terms of mass, shape, size, density, and chemical properties.

Split-flow thin (SPLITT) cell Fractionation (SF) is a family of techniques that can be employed to separate particles and macromolecules into two or more subpopulations.³⁻⁹ SF has been used for separation and analysis of various materials including proteins,^{7,10-13} micron-size glass beads,^{8,14} starch,^{14,15} drug-carrying liposomes,¹⁶ cells,¹⁷⁻¹⁹ silica and synthetic diamond particles,²⁰ magnetic particles,²¹ and various environmental particles.²²⁻²⁴

SF is carried out in a thin ribbon-like channel (0.1-1 mm thick) equipped with splitters at the inlet and the outlet of the channel, across which an external field is applied. The expanding view of the basic SPLITT channel is shown schematically in Figure 1. There are two inlets and two outlets separated by the inlet and outlet splitters as shown in Figure 1. In normal operation of SF, the sample substream is fed into the inlet-*a'* at the flow rate of $V(a')$ while the carrier liquid is fed into the inlet-*b'* at the flow rate of $V(b')$. The upper broken line in Figure 1 labeled "inlet splitting plane (ISP)" denotes the imaginary line dividing the two inlet substreams. Generally the two inlet flow rates are set in such a way that $V(b')$ is higher than $V(a')$, compressing the sample substream near the top wall. Thus the incoming sample flowstream is initially confined to a narrow layer called "sample-feed

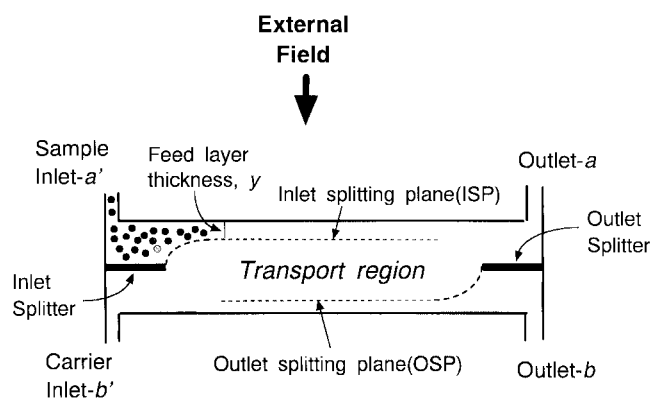


Figure 1. Schematic view of a SF channel. Particles mobile enough to cross the outlet splitting plane (OSP) exit outlet-*b*, the remainder outlet-*a*.

layer" above the ISP. The substreams *a'* and *b'* merge as soon as they pass beyond the edge of the inlet splitter. During passage down the channel, sample components interact with the external field and are forced to migrate laterally (toward the bottom of the channel). When the fluid stream reaches the outlet splitter, it is divided into two fractions by the outlet splitter. The lower broken line labeled "outlet splitting plane (OSP)" denotes the line separating the two outlet flows. The function of the outlet splitter is to direct the flow streams above and below the OSP into the appropriate outlets. Sample components migrating fast enough to cross the OSP will exit the outlet-*b*, and the rest will exit the outlet-*a*, providing separation of the particles into two fractions. Whether a given particle exits the outlet-*a* or *b* depends on the position of OSP, which is determined by the relative flow rates of the substreams emerging from outlet-*a* and *b*, termed $V(a)$ and $V(b)$, respectively.

SF is non-destructive as the sample components are under

very little mechanical stress, if any, during GSF operation. SF theory is relatively straightforward because SF channel flow is a laminar and has simple parabolic flow profile in thin rectangular cross section. This theoretical simplicity allows direct calculation of separation parameters (e.g., content of oversized particles¹⁴ and the macromolecular diffusion coefficient.¹¹) from SF data. Generally the SF process is rapid (~1 min) because the SF channel is thin. Also the SF process is highly flexible because the sample transport is governed by the adjustable field strength and by the positions of the ISP and OSP, which are controlled by the ratios of the flow rates entering the inlet and outlet of the channel, $V(a')$ and $V(b')$. Throughput is also easily adjusted as it increases with the applied field strength and with the area of the flow cell and the flow rates. The resolution in SF is relatively high because there is no convective flow along the separation path. SF is applicable to various particulate samples because there is no limit on carrier solvent. The most important merit of SF is it can be operated continuously, and thus the quantity of material fractionated can be increased in proportion to the operating time.

There are a few subtechniques of SF based on the type of the external field employed, which include gravitational SF (GSF), centrifugal SF (CSF), electrical SF (ESF), and diffusion mode SF. GSF uses earth's gravity as the external field, and has been mainly used for the separation of particles of a few microns or larger.^{4,8,14,15,18-24} CSF uses centrifugal force, and extends the capabilities of GSF to materials in the colloidal size range and to particles of low density. CSF has been used for separation of human blood cells and proteins¹² and various colloidal particles.²⁵ ESF uses an electrical field,²⁶ and has been used for separation of charged proteins.⁷ The diffusion mode SF has been used for separation of various proteins.^{10,11,13,16,17} In this work, a GSF system was assembled and tested using polystyrene latex particles. Then the GSF system was tested for its applicability to separation of environmental particles such as dust and ground water particulates.

Theory

In GSF, the lateral migration velocity (settling velocity) U of a particle toward the bottom of the channel is determined by the sedimentation coefficient s , and is given by⁴

$$U = s G \quad (1)$$

where G is the field-induced acceleration due to the earth's gravity. For spherical particles, the sedimentation coefficient s is given by^{4,8,27,28}

$$s = \frac{\Delta\rho d^2}{18\eta} \quad (2)$$

where $\Delta\rho$ is the density difference between the particle and the carrier liquid, d the particle diameter, and η the viscosity of the carrier liquid. It can be seen that the sedimentation coefficient is proportional to the product $\Delta\rho d^2$ or d^2 if all particles have the same density.

The volumetric flow elements crossed by a particle during its transport process in SF channel, ΔV , is given by⁴

$$\Delta V = bLU, \quad (3)$$

where b and L are the thickness and the length of the channel, respectively. In a GSF channel, ΔV increases with U , and thus with the sedimentation coefficient s .

The region sandwiched between the ISP and the OSP is called the "transport region" or "transport layer". The volumetric flow rate of the transport region $V(t)$ is expressed by⁴

$$V(t) = V(a) - V(a') = V(b') - V(b) \quad (4)$$

In an ideal case when the thickness of the sample-feed layer, y , is so small that all particles enter the channel in the same stream plane, particles are divided into two groups depending on their ΔV values.^{4,14,25} Particles whose ΔV is larger than $V(t)$ exit the outlet- b , and thus the retrieval factor, F_b (the fraction of particles recovered from outlet- b) = 1. Particles with ΔV smaller than $V(t)$ exit the outlet- a ($F_b=0$). When all particles have the same density, it results in a separation of the sample population into two fractions having diameters above or below the cutoff diameter d_c . The cutoff diameter d_c is given by^{4,14,25}

$$d_c = \sqrt{\frac{18\eta V(t)}{bLG\Delta\rho}} \quad (5)$$

The cutoff diameter d_c can be readily controlled in GSF by varying the flow rates that determine $V(t)$.

In reality, the sample-feed layer has a finite thickness, which is determined by the ratio of the two incoming flow rates, $V(a')$ and $V(b')$. If the particles arrive at the end of the inlet-splitter uniformly distributed over the sample-feed layer, particles are divided into three groups depending on their ΔV values.^{4,8,9,25} Particles having ΔV larger than $V(a)$ exit the outlet- b ($F_b=1$) while those having ΔV smaller than $V(t)$ exit the outlet- a ($F_b=0$). The third group contains particles having ΔV larger than $V(t)$ but smaller than $V(a)$, $V(t) < \Delta V < V(a)$. They have F_b values ranging between 0 and 1, meaning the particles exit both outlets even if they have the same diameter. For this group of particles, following equation applies;

$$F_b = \frac{\Delta V - V(t)}{V(a')} \quad \text{when } V(t) < \Delta V < V(a) \quad (6)$$

If $V(t)$ is expressed by eq. 4, eq. 6 becomes

$$F_b = \frac{\Delta V + V(a')}{V(a')} - \frac{V(a)}{V(a')} \quad (7)$$

With $V(a')$ held constant, F_b is inversely proportional to $V(a)$. If we define the cutoff diameter, d_c as the diameter at which 50% of the particles exit outlet- b ($F_b=0.5$),

$$d_c = \sqrt{\frac{18\eta}{bLG\Delta\rho} (V(t) + 0.5V(a'))} \quad (8)$$

is obtained.²⁵ As a result, SF operation separate particles into two fractions at or around a cutoff diameter, d_c . The cutoff

diameter d_c can be again readily controlled in GSF by varying the flow rates that determine $V(t)$. For the best separation resolution, $V(b')$ must be much larger than $V(a')$, so that the thickness of the sample feed-layer becomes very small.

Experimental Section

GSF System. The GSF channel used in this study is constructed by sandwiching a stainless steel sheet (0.0127 cm thick) between two Lucite blocks as shown in Figure 2. The channel shapes (shaded area in Figure 2) are machined out from the inside faces of the Lucite blocks to form the channel. The depth of the machined area is 0.0127 cm. A rectangular section is also cut out from the stainless steel sheet that defines the rectangular shape of the SF channel. The resulting SF channel has dimensions of 0.0381 cm in thickness, 4 cm in breadth, and 20 cm in length between the edges of two splitters. Two pumps delivered two independent flows to the inlet- a' and b' , respectively. The Gilson Minipuls 3 peristaltic pump (Gilson Medical Electronics, Middleton, WI, USA) provided the flow to the inlet- a and the Young-Lin M930 piston pump (Young-Lin Science, AnYang, Korea) provided the flow to the inlet- b' . The sample is fed into the SF channel by two different methods (injection mode or continuous mode). For the injection mode, sample suspension is directly injected through a septum placed in the inlet- a' using a syringe. For continuous mode, the sample suspension is continuously fed into the channel from a magnetically stirred vial placed between the peristaltic pump and the connection to the inlet- a' . The two outlet flow rates, $V(a)$ and $V(b)$, are controlled by using the backpressure provided by tubing of various diameters and lengths. In order to monitor the particulate content of the emerging streams, two UV/VIS detectors are connected to the outlet- a and b , a Young-Lin M720 UV/VIS detector to the outlet- a and a Gilson 112 UV/VIS detector to the outlet- b , respectively. Both detectors were operated at 254 nm. The fraction of particles emerging from the outlet- b , F_b was calculated by

$$F_b = \frac{A(b)V(b)}{A(a)V(a) + A(b)V(b)} \quad (9)$$

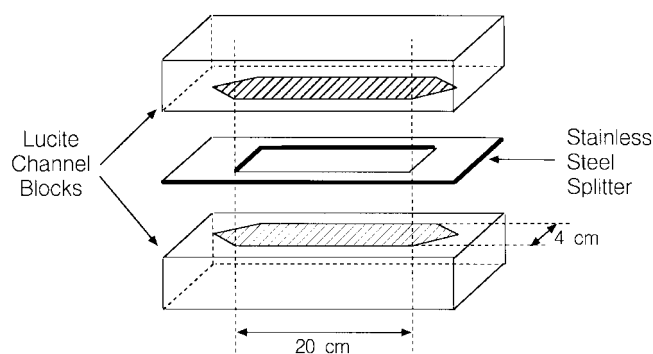


Figure 2. Diagram of SF channel assembly.

where $A(a)$ and $A(b)$ are peak areas of the detector response curves at outlet- a and b , respectively. As the two detectors connected to two outlets are different, their responses are normalized before determining F_b by measuring the ratio between the peak areas obtained from two detectors after connecting them in series.

The carrier fluid was an aqueous solution of 0.1% (w/v) FL-70 (Fisher Scientific, Fair Lawn, NJ, USA) and 0.02% (w/v) sodium azide (NaN_3). For calculation purposes, viscosity and density of the carrier-fluid are taken to be 0.01 poise and 1.00 g/mL, respectively. The GSF system was maintained at room temperature during operation.

Polystyrene Latex Beads and Environmental Particulates. Spherical polystyrene (PS) latex particles of 9.8 and 21.4 μm in diameter were obtained as 10% suspensions from Duke Scientific Corporation (Palo Alto, CA, USA). The particles have the density of 1.05 g/mL and a 16.3% and 15.0% coefficient of variation for 9.8 and 21.4 μm particles respectively. Dust particles are collected at the top of the laboratory building of the Korea Institute of Geoscience and Mineral Resources (KIGAM) using a High Volume Sampler (Kimoto PM-10). Dust particles are dispersed in the carrier solution in a bath sonicator. The groundwater sample is collected in the area near the town of Mun-Kyung, Korea.

Microscopy. An optical microscopy (CARLZEISS JENA, Laboval 4) was used to take pictures of particles. A scanning electron microscopy (JEOL JSM 6400, Tokyo, Japan) equipped with a NORAN instrument's Energy Dispersive X-ray (EDX) instrument (Baker Hughes Company, Middleton, WI, USA) was used for surface analysis of particles.

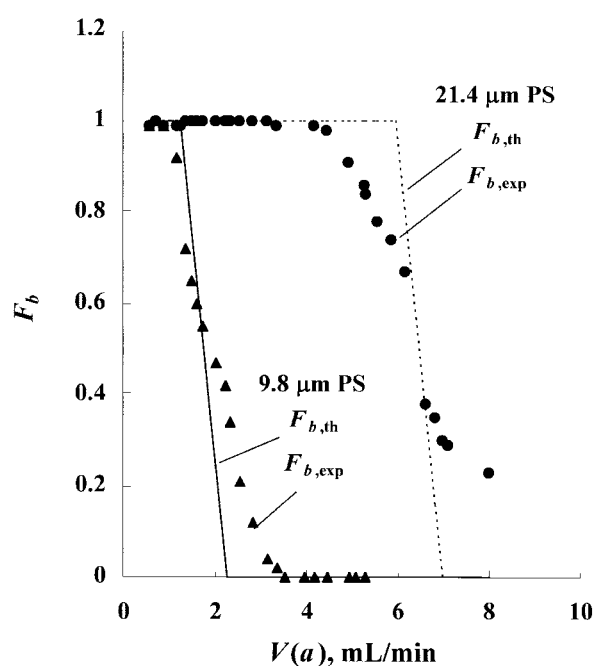


Figure 3. F_b vs. $V(a)$ for 9.8 and 21.4 mm polystyrene latex particles with $V(a')=V(b)=1.0$ mL/min. The circles and triangles are experimental data (determined by eq. 6), and the broken and solid lines are theoretical plots (calculated using eq. 7).

Results and Discussion

Separation of 9.8 and 21.4 μm Polystyrene Latex Particles. The newly assembled GSF system is tested using polystyrene latex particles. Figure 3 shows theoretical and experimental plots of F_b vs. $V(a)$ obtained for 9.8 and 21.4 μm polystyrene latex particles. $V(a')$ was kept constant at 1 mL/min. In all experiments, $V(b) = V(a')$ and $V(b') = V(a)$. The circles and triangles are F_b values determined experimentally for each polystyrene particle sample from eq. 9, and the solid and broken lines are theoretical plots calculated using eq. 7 for 9.8 and 21.4 μm polystyrene particles respectively. As discussed earlier, theoretical plots show the presence of three discrete regions. In the first region, where $V(a)$

is relatively low, F_b remains at 1 regardless of $V(a)$ and all particles exit the outlet- b . In the second region, F_b decreases linearly from 1 to 0 ($0 < F_b < 1$) as $V(a)$ increases and the particles exit both outlets a and b even though all particles have the same size and density (thus the same sedimentation coefficient). In the final region, where $V(a)$ is relatively high, F_b remains at 0 regardless of $V(a)$ and all particles exit the outlet- a . The presence of the second region ("transition region") is due to the sample-feed layer having a finite thickness. If the sample-feed layer is so narrow that the layer thickness is negligible, all particles enter the channel in the same stream plane, and there exist no such transition region. Then only two regions exist where F_b is either 1 or 0 and F_b drops vertically from 1 to 0. Practically it is impossible to

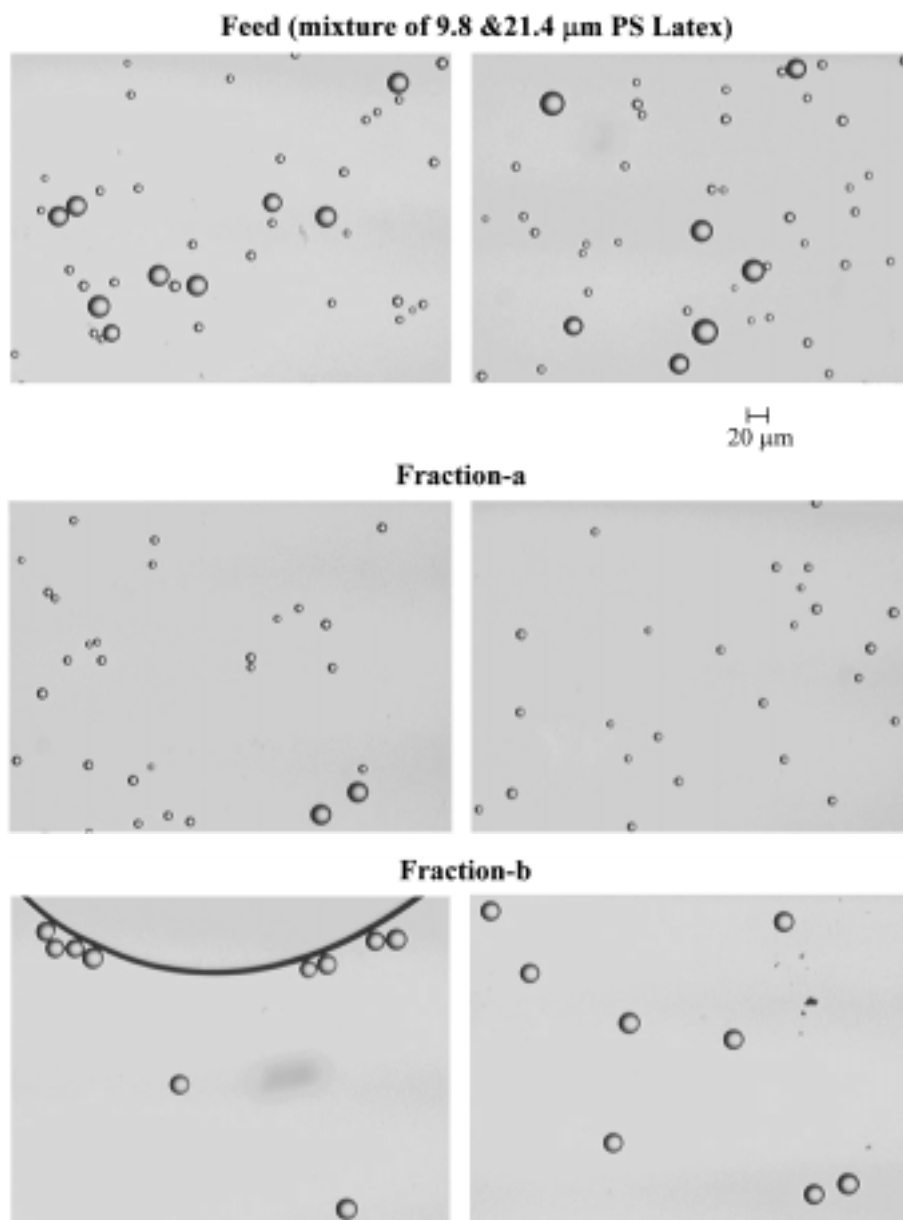


Figure 4. Optical micrographs ($\times 100$) of a mixture of 9.8 and 21.4 μm PS particles (top), fractions- a (middle), and fraction- b (bottom) obtained at $V(a')=V(b)=1.0$ mL/min and $V(b')=V(a)=4.1$ mL/min.

avoid the presence of the transition region completely. Efforts should be made to narrow the thickness of the sample-feed layer so that the transition from $F_b=1$ to 0 becomes as sharp as possible. As seen in eq. 7, the slope of the F_b vs. $V(a)$ plot is $-(1/V(a'))$. As $V(a')$ decreases, the negative slope of the plot increases, and the transition from $F_b=1$ to 0 becomes sharper.

Experimental data show reasonable agreements with theory for both 9.8 and 21.4 μm polystyrene particles, although the transition from $F_b=1$ to 0 is not as sharp as predicted by theory. Possible reasons for this discrepancy include the mixing of flow streams, flow turbulence at the edges of the splitters, geometrical imperfections, etc. Also in theoretical calculations, the polystyrene particles are assumed to be monodisperse although the 9.8 and 21.4 μm particles are

listed as having a 16.3% and 15.0% coefficient of variation respectively. Theory predicts the transition from $F_b=1$ to 0 becomes sharper as $V(a')$ decreases. Experimental results at lower $V(a')$ did not show much improvement in the agreement with theory.

To separate 9.8 and 21.4 μm polystyrene latex particles, an appropriate combination of $V(a')$, $V(b')$, $V(a)$, and $V(b)$ must be found, where all 21.4 μm particles exit the outlet-*b*, while all 9.8 μm particles exit the outlet-*a*. Figure 3 indicates there is a range of $V(a)$ between about 3.5 and 4.5 mL/min, where this requirement will be met. A continuous GSF operation was performed for a mixture of 9.8 and 21.4 μm polystyrene particles with the flow rates $V(a') = V(b) = 1.0$ mL/min and $V(b') = V(a) = 4.1$ mL/min respectively. Figure 4 shows optical micrographs of the feed-mixture of the two polysty-

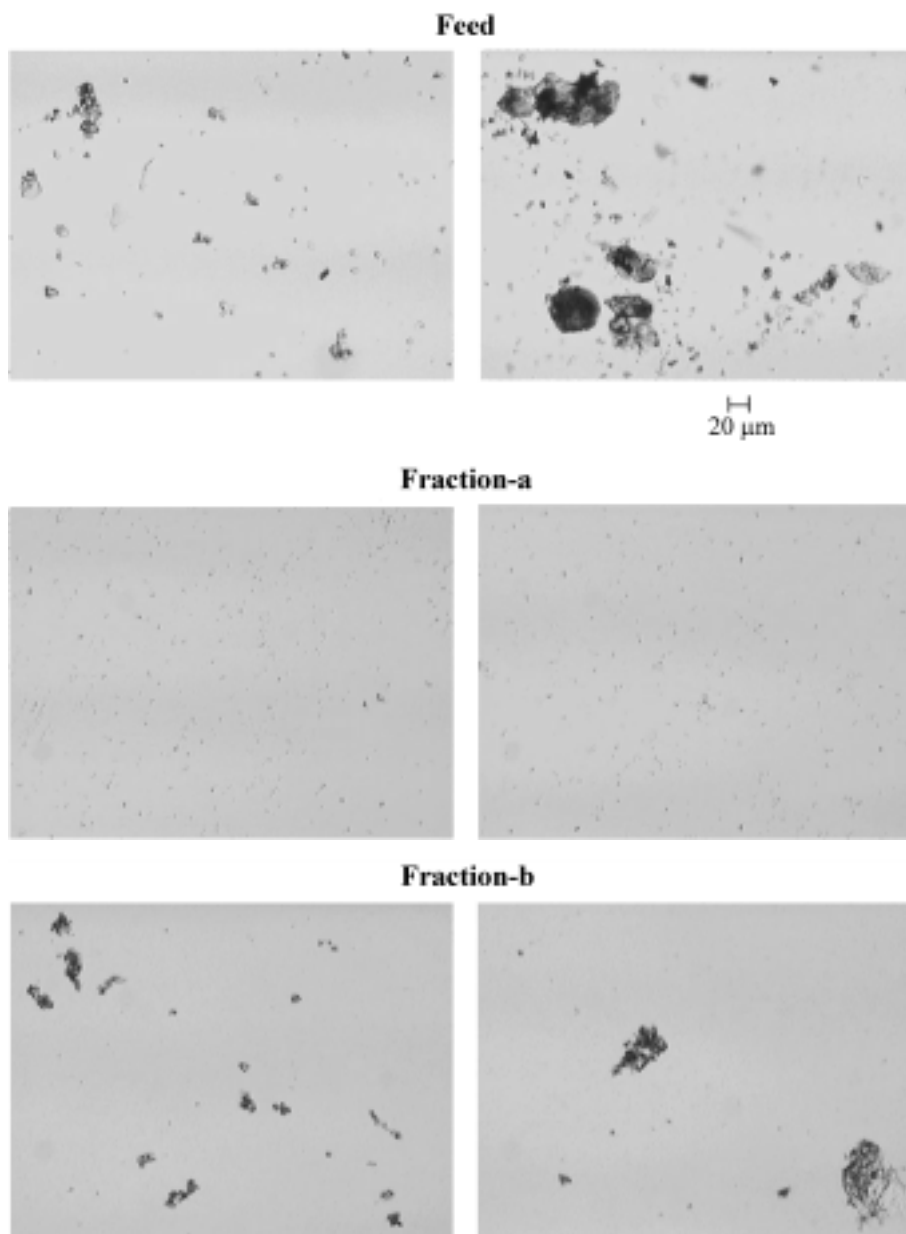


Figure 5. Optical micrographs ($\times 100$) of dust (top), fractions-*a* (middle), and fraction-*b* (bottom) obtained at $V(a')=V(b)=0.40$ mL/min, and $V(b')=V(a)=0.12$ mL/min.

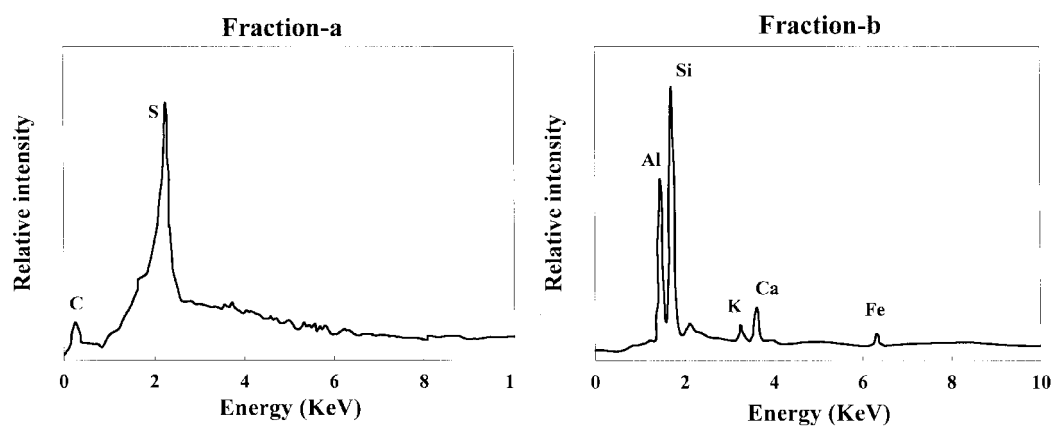


Figure 6. SEM-EDX data of fraction-*a* and *b* of dust particles shown in Figure 5.

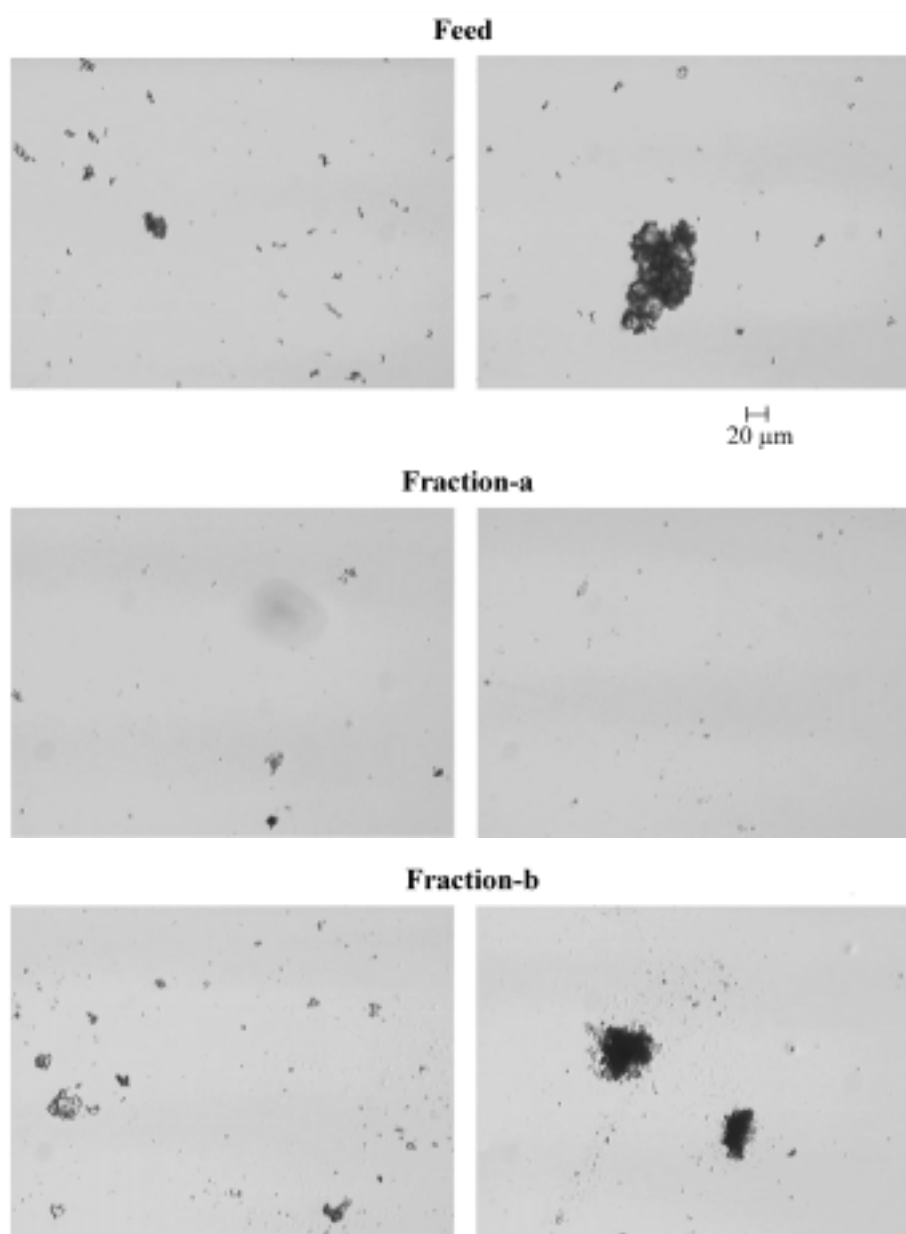


Figure 7. Optical micrographs (×100) of ground water particles (top), fractions-*a* (middle), and fraction-*b* (bottom) obtained at $V(a')=0.25$, $V(b')=2.0$, $V(a)=0.37$, and $V(b)=1.88$ mL/min, respectively.

rene particles and the fractions collected from the outlet-*a* and the outlet-*b*. All the micrographs were obtained at 100-times magnification. As shown in Figure 4, a successful separation is obtained with a slight contamination observed in the fraction-*a*.

Separation and Characterization of Dust particles. In order to apply the GSF system for analysis of dust particles, various combinations of four flow rates ($V(a')$, $V(b')$, $V(a)$, and $V(b)$) are tested to find a condition where about 50% of the dust particles exit the outlet-*a* and the rest the outlet-*b* so that F_b becomes about 0.5. Figure 5 shows optical micrographs of the original dust particles, fraction-*a*, and fraction-*b* collected at the flow rates of $V(a')=V(b)=0.40$ mL/min, and $V(b')=V(a)=0.12$ mL/min. The magnification was the same as before. The fraction-*a* contains small particles, while the fraction-*b* contains relatively larger particles, as expected. Figure 6 shows SEM-EDX data obtained for the dust particles in the fraction-*a* and fraction-*b*. It can be seen that the particles contained in the fraction-*a* are composed mostly of C (carbon) and S (sulfur). Those in the fraction-*b* are composed mostly of Al, Si, K, Ca and Fe, which are typically found in sand or soil.

Separation of Underground Water. The GSF system is also tested for its applicability to separation of particles in ground water. This time $V(a')$ and $V(b')$ are fixed constant at 0.25 and 2.00 mL/min respectively so that the total incoming flow rate and the flow rate ratio $V(b')/V(a')$ are held constant at 2.25 mL/min and 8, respectively. While keeping $V(a')$ and $V(b')$ constant, $V(a)$ and $V(b)$ are varied to find a condition where F_b becomes around 0.5. Figure 7 shows Optical micrographs (100) of the particles in the ground water and in the fraction-*a* and *b* obtained at $V(a')=0.25$, $V(b')=2.00$, $V(a)=0.37$, and $V(b)=1.88$ mL/min, respectively. The micrographs show a successful separation of the ground water particles based on the size.

Summary. GSF showed a high potential for a large-scale separation of complex environmental particles contained in dust or ground water into subpopulations, which can be further analyzed independently by other analytical techniques. GSF is relatively inexpensive to build, and its performance is predictable due to theoretical simplicity and the good agreement between theory and experiment. More work toward further optimization of the GSF instrument is needed to remove probable causes (flow-turbulence at the edges of the splitters and the geometrical imperfections, etc) of the discrepancy between theory and experimental data. Combining GSF with other techniques such as field-flow fractionation (FFF) or ICP/MS will provide a powerful tool for separation and accurate analysis of particulates including various environmental particles.

Acknowledgment. This work was supported financially by a research grant from the Hannam University.

References

1. Stumm, W.; Morgan, J. J. *Aquatic Chemistry*; Wiley: New York, 1981.
2. Pickup, G. In *The role of Particulate Matter in the Transport and Fate of Pollutants*; Hart, B. T., Ed.; Water Studies Center: Melbourne, 1986; Chapter 3, p 97.
3. Giddings, J. C. *Sep. Sci. Technol.* **1985**, 20(9&10), 749.
4. Springston, S. R.; Myers, M. N.; Giddings, J. C. *Anal. Chem.* **1987**, 59, 344.
5. Giddings, J. C. *Sep. Sci. Technol.* **1988**, 23(1-3), 119.
6. Giddings, J. C. *Sep. Sci. Technol.* **1988**, 23(8&9), 931.
7. Levin, S.; Myers, M. N.; Giddings, J. C. *Sep. Sci. Technol.* **1989**, 24(14), 1245.
8. Gao, Y.; Myers, M. N.; Barman, B. N.; Giddings, J. C. *Particulate Science and Technology* **1991**, 9, 105.
9. Giddings, J. C. *Sep. Sci. Technol.* **1992**, 27(11), 1489.
10. Williams, P. S.; Levin, S.; Lenczycki, T.; Giddings, J. C. *Ind. Eng. Chem. Res.* **1992**, 31, 2172.
11. Fuh, C. B.; Levin, S.; Giddings, J. C. *Analytical Biochemistry* **1993**, 208, 80.
12. Fuh, C. B.; Giddings, J. C. *Biotechnol. Prog.* **1995**, 11, 14.
13. Fuh, C. B.; Giddings, J. C. *Sep. Sci. Technol.* **1997**, 32(18), 2945.
14. Fuh, C. B.; Myers, M. N.; Giddings, J. C. *Anal. Chem.* **1992**, 64, 3125.
15. Contado, C.; Riello, F.; Dondi, F. *7th International Symposium on Field-Flow Fractionation*; University Park Hotel, Salt Lake City, Utah, USA, 1998.
16. Levin, S.; Tawil, G. *Anal. Chem.* **1993**, 65, 2254.
17. Levin, S.; Giddings, J. C. *J. Chem. Tech. Biotechnol.* **1991**, 50, 43.
18. Zhang, J.; Williams, P. S.; Myers, M. N.; Giddings, J. C. *Sep. Sci. Technol.* **1994**, 29(18), 2493.
19. Fuh, C. B.; Trujillo, E. M.; Giddings, J. C. *Sep. Sci. Technol.* **1995**, 30(20), 3861.
20. Jiang, Y.; Kummerow, A.; Hansen, M. *J. Micro Sep.* **1997**, 9, 261.
21. Jiang, Y.; Miller, M. E.; Hansen, M. E.; Myers, M. N.; Williams, P. S. *J. Magnetism and Magnetic Materials* **1999**, 194, 53.
22. Keil, R. G.; Tsamakis, E.; Fuh, C. B.; Giddings, J. C.; Hedges, J. I. *Geochimica et Cosmochimica Acta* **1994**, 58(2), 879.
23. Contado, C.; Dondi, F.; Beckett, R.; Giddings, J. C. *Analytica Chimica Acta* **1997**, 345, 99.
24. Dondi, F.; Contado, C.; Blo, G.; Garcia Martin, S. *Chromatographia* **1998**, 48(9/10), 643.
25. Fuh, C. B.; Myers, M. N.; Giddings, J. C. *Ind. Eng. Chem. Res.* **1994**, 33(2), 355.
26. Giddings, J. C. *J. Chromatogr.* **1989**, 480, 21.
27. Jiang, Y.; Hansen, M.; Gidding, J. C. *Proceedings of the 5th World Congress of Chemical Engineering* **1996**, 465.
28. Gupta, S.; Ligrani, P. C.; Giddings, J. C. *Sep. Sci. Technol.* **1997**, 32(10), 1629.